X-ray scattering from misfit dislocations in heteroepitaxial films: The case of Nb(110) on Al_2O_3

R. I. Barabash,[a] W. Donner, and H. Dosch[b]
Max-Planck-Institut für Metallforschung, D-70569 Stuttgart, Germany
and Institut für Theoretische und Angewandte Physik, Universität Stuttgart, D-70569 Stuttgart, Germany

(Received 23 August 2000; accepted for publication 30 November 2000)

We apply the Krivoglaz theory of x-ray scattering to thin epitaxial films containing misfit dislocations and reanalyze the seemingly puzzling x-ray scattering phenomena observed in several heteroepitaxial films. We show that the two-line shape scattering distribution and its dependence upon film thickness and momentum transfer can be understood in natural way and on a quantitative level. Extended diffuse x-ray scattering maps have been obtained from $Nb(110)/Al_2O_3(11\bar{2}0)$ which are discussed within the framework of this theory disclose a particular dislocation network at the $Nb-Al_2O_3$ interface. © *2001 American Institute of Physics.* [DOI: 10.1063/1.1342215]

Thin films grown heteroepitaxially on single crystal substrates are the elementary building blocks for nanotechnology, consequently, a lot of effort has been devoted to detailed understanding of their microscopic structure. The real structure of these systems is generally complicated, since the unavoidable lattice mismatch between the film and the substrate gives rise to elastic strain and strain relaxation processes by introducing misfit dislocations at the film–substrate interface.

A classical system in metal epitaxy is Nb/Al_2O_3, which is extensively used as a template for the growth of metal films and superlattices. Consequently, the real structure of epitaxial Nb has been the focus of scientific interest for a couple of years. Several x-ray diffraction[1–3] and high resolution transmission electron microscopy (TEM) studies[4] have been performed however, despite of all this experimental effort, the defect structure in epitaxial Nb is still somewhat unclear; furthermore, the associated x-ray diffraction profiles from epitaxial Nb films seem to exhibit rather unusual and puzzling features.[2]

The TEM studies of $Nb(110)-Al_2O_3(11\bar{2}0)$ give clearcut evidence of a dislocation network at the film–substrate interface (Fig. 1), however, they leave some ambiguity between two possible network structures, denoted A and B in Fig. 1 (for further explanation and notations see Fig. 1). All x-ray diffraction studies have focused on the transverse line shapes across $(hh0)$ reciprocal lattice vectors (see the inset of Fig. 2). A recent result for the transverse (110) and (220) diffraction profile is shown in Fig. 2 and was obtained by us for a 190 Å thick Nb(110) film and shows, as also observed by others,[1,2] two components with rather different widths and intensities. This peculiar two-component structure has also been observed in many other heteroexpitaxial systems such as in ErAs grown on InGaP.[5–7] It has been noted by all the authors that this two-component structure exhibits rather unexpected behavior versus film thickness (L_z) and x-ray momentum transfer ($\mathbf{Q}$), *inter alia*: the sharp Bragg component disappears with growing film thickness, accompanied by narrowing of the broad component.[2] One successful theoretical treatment of misfit dislocation-mediated x-ray scattering was presented recently for the extreme cases of very low and very high dislocation density.[8] It can not however, be applied to the intermediate cases discussed here nor can it rationalize the puzzling thickness dependence of the scattering phenomena.

In this work we determined the actual dislocation network from extended diffuse x-ray diffraction maps. We further show that an extension of the Krivoglaz theory of x-ray scattering from bulk crystals containing dislocations to the situation of misfit dislocations in thin epitaxial films allows one to understand all hitherto puzzling x-ray observations in a quantitative and self-consistent way.

Following the work of Krivoglaz[9] we subdivide the total x-ray scattering intensity $I(Q)$ from epitaxial films into a sharp Bragg component (I_0) and a broad diffuse component (I_D). In thin film geometry they are

$$I_0(\mathbf{Q})=\frac{|f|^2N}{\nu^2V}e^{-2W}\sum_G \delta(\mathbf{q}_\parallel)\frac{\sin^2(q_zL_z/2)^2}{(q_z/2)^2}, \tag{1}$$

and

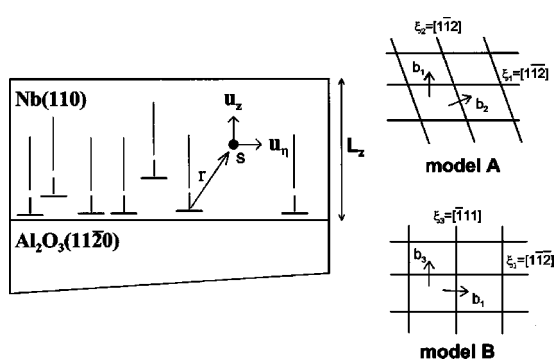

FIG. 1. Left: Sketch of misfit dislocation in a thin film on a substrate, giving rise to distortion fields u_η, u_z at point **s**. Right: Possible dislocation networks of $Nb(110)/Al_2O_3$; model A contains Burgers vectors $b_1=\frac{1}{2}[1\bar{1}1]$, $b_2=\frac{1}{2}[\bar{1}11]$, model B consists of $b_3=\frac{1}{2}[\bar{1}1\bar{2}]$.

[a]Permanent address: Kiev Polytechnical Institute, National Technical University Ukraine, Pr. Pobedy 37, UA-252056 Kiev, Ukraine.
[b]Electronic mail: dosch@dxray.mpi-stuttgart.de

 © 2001 American Institute of Physics
Downloaded 06 Sep 2009 to 160.91.157.167. Redistribution subject to AIP license or copyright; see http://apl.aip.org/apl/copyright.jsp

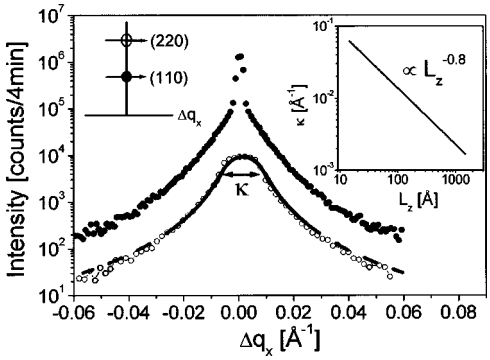

FIG. 2. Rocking scans through the (110) and (220) reflections as a function of q_x (see the inset on the left). The straight line through the center of the (220) reflection is based on Eq. (2), and the tails (dashed curves) follow $1/q^3$ behavior arising from the dislocation cores. The inset on the right shows the calculated half widths κ as a function of the film thickness.

$$I_D(\mathbf{Q})=|f|^2\sum_{ss'}^{L_z} e^{-2W}\exp(i\mathbf{q}(\mathbf{R}_s^0-\mathbf{R}_{s'}^0))e^{-(T-T_\infty)}, \quad (2)$$

with $\mathbf{q}=\mathbf{Q}-\mathbf{G}_{hkl}$ as the deviation from the reciprocal lattice vector $\mathbf{G}_{hkl}$. f is the scattering amplitude of the atoms within the unit cell at positions $\mathbf{R}_s^0$ of the undistorted reference (thin-film) crystal with thickness L_z and volume V. As we will see below, the thin-film behavior of the functions $2W$, T_1 and T_∞ which occur in Eqs. (1) and (2) require most careful consideration: The complex function $T=T_1+iT_2$ is given by[9]

$$T_1=\sum_t c\{1-\cos[(\mathbf{R}_{ss'}\nabla)(\mathbf{Q}u_{st})]\},$$
$$T_2=\sum_{t_\alpha} c(\mathbf{R}_{ss'}\nabla)(\mathbf{Q}u_{st}), \quad (3)$$

and determined by the lattice distortions u_{st} associated with the presence of dislocations of concentration c (see Fig. 1). The summation is performed over all dislocation positions t and all possible dislocation networks within the epitaxial film $(\mathbf{R}_{ss'}=\mathbf{R}_s-\mathbf{R}_{s'})$. The asymptotic value (static Debye–Waller factor),

$$2W=Re(T_\infty)=c\cdot\lim_{R_{ss'}^0\to\infty}\sum_t[1-\cos(\mathbf{Q}(u_{st}-u_{st'})], \quad (4)$$

which appears in Eqs. (1) and (2) governs the lattice distortion-induced intensity redistribution between the sharp Bragg and the diffuse broad scattering component. For given lattice distortions u_{st} the diffuse x-ray scattering and the damping of the Bragg component can be calculated numerically using Eqs. (1)–(4). In the case of misfit dislocation networks of either type A or B (see Fig. 1) the in-plane and out-of-plane lattice distortions (associated with one dislocation) are given by[8,10,11]

$$u_\eta=\frac{b}{2\pi}\left[\frac{1}{\tan(z/x)}+\frac{xz}{2(1-\mu)(x^2+z^2)}\right],$$

and

$$u_z=-\frac{b}{8\pi(1-\mu)}\left[(1-2\mu)\ln(x^2+z^2)+\frac{x^2-z^2}{x^2+z^2}\right], \quad (5)$$

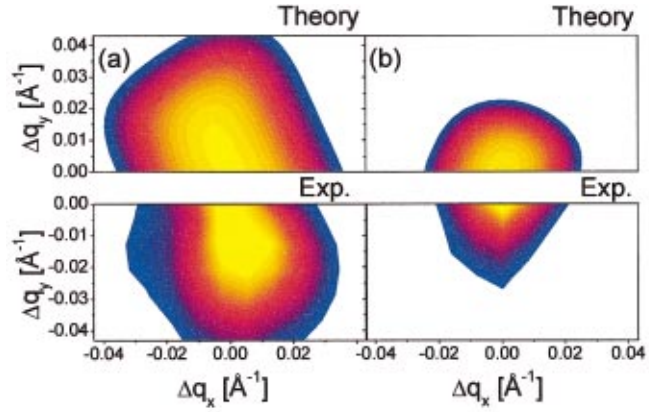

FIG. 3. (Color) Diffuse intensity distribution around the Nb(110) reflection in the plane perpendicular to the surface normal for a (a) 50 and (b) 190 Å thick Nb film. The upper parts show calculations based on Eqs. (1)–(4), and the lower parts display experiments. The color scales represent intensities on a logarithmic scale.

respectively[12] (with b as the Burgers vector and μ as the Poisson ratio). Notice here that, due to the special arrangement of the misfit dislocations under consideration, the diverging $\ln(r)$-distortion field (u_z) is directing along the film normal, thus, it is truncated by the finite thickness of the epitaxial film. We will show in what follows that these ingredients are sufficient to explain all experimental findings on a quantitative level.

We first turn to the broad diffuse x-ray diffraction component: We experimentally mapped the diffuse scattering in an extended (q_x-q_y)-plane (parallel to the surface) around the Nb(110) reflection (these diffraction experiments were carried out at HASYLAB beamline BW6). Figure 3 shows by way of example the experimental results for a 50 and a 190 Å thick Nb(110) film together with theoretical simulations based on Eq. (2) using the lattice distortions [Eq. (5)] associated with misfit dislocation networks A and B, respectively. We already find good quantitative agreement between experiment and theory, if we assume that the diffuse intensity pattern is predominantly mediated by a dislocation network of type B; the best fit, however, is achieved by also allowing 5% secondary dislocations of type A. This theoretical model of diffuse scattering explains all reported features of the broad component quantitatively, as demonstrated in Fig. 2: The calculated diffuse scattering (full curve) exhibits the experimentally observed width and line shape. Our predictions for its dependence of the line shape upon the film thickness is shown in the inset on the right which indeed discloses the reported narrowing phenomenon. Notice here that the width of the diffuse scattering finally converges to the bulk scattering profile, which is often referred to as ''broadening of the Bragg reflections.'' [13] From the comparison between the experimental and calculated diffuse maps we deduce a linear misfit dislocation density $c=N/L_x$ of $1.5\times10^6\ \mathrm{cm}^{-1}$ along the (112) direction (N is the number of dislocations and L_x an in-plane length).

We now turn to the (resolution-limited) sharp Bragg component: Its integrated intensity is given by the static Debye–Waller factor (DWF) $\exp(-2W)$ [Eq. (2)]. As one knows, $\exp(-2W)=0$ in bulk systems in the presence of dislocations (defect of the second kind) above a critical concen-

Downloaded 06 Sep 2009 to 160.91.157.167. Redistribution subject to AIP license or copyright; see http://apl.aip.org/apl/copyright.jsp

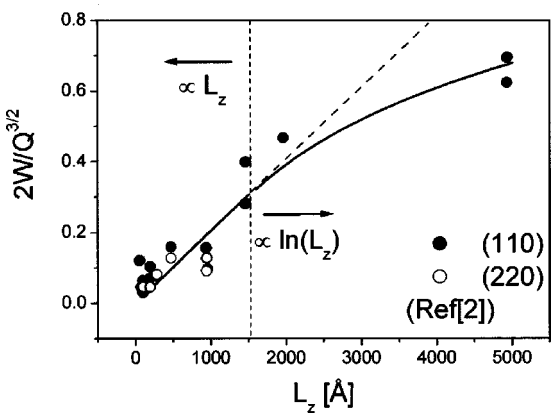

FIG. 4. Damping of the peak intensities as a function of the film thickness. Experimental data (closed and open symbols) were taken from Ref. 2, and the solid line represents a crossover from linear to logarithmic behavior.

tration n_c, thus, the sharp component disappears (and is replaced by a broader component with the aforementioned narrow width). This is caused by the (infinite) summation in Eq. (4) which diverges for ln(r)-type distortions; however, in thin films, the summation is truncated by the finite thickness of the film rendering $2W$ finite and, thus, $\exp(-2W)\neq 0$. This qualitative argument already explains the additional presence of the resolution-limited sharp component in thin films as seen in the two-line shape profiles (Fig. 2). A more detailed analysis of the epitaxial static Debye–Waller factor $2W$ associated with misfit dislocations gives, in leading order,

$$2W \propto c \cdot Q^{3/2} \begin{cases} L_z/a: & L_z \ll L_x, \\ \ln(L_z/a): & L_z \gg L_x, \end{cases} \tag{6}$$

which scales with $Q^{3/2}$ (i.e., in non-Gaussian behavior!) and with film thickness (as reported), thereby showing a crossover between thin-film and thick-film limiting behavior. Interestingly, it turns out that the crossover thickness depends on the lateral length scale L_x given by the lateral coherence length of the x rays and/or the lateral growth coherence of the Nb film. Figure 4 shows a comparison of Eq. (6) with the reported experimental results for the (110) and (220) reflections reported by Wildes *et al.*[2] assuming a lateral coherence length of the order of 1.5 μm (associated with the given q resolution $\Delta q = 0.0045\,\text{Å}^{-1}$). The thin-film DWF ($2W \propto L_z$) is expected for $L_z \ll L_x$, i.e., in practice for $L_z \approx L_x/10 = 1500\,\text{Å}$ (vertical dashed line in Fig. 4). This is readily observed as demonstrated by the excellent quantitative agreement between our theoretical prediction (solid line) and the reported values. Thus, we suggest that the phenomenological powerlaw behavior $2W = L_z^{0.68}$ put forward in Ref. 2 is in fact crossover behavior from $2W \propto L_z$ for small film thicknesses to $2W \propto \ln L_z$ for thicker films. Also shown in Fig. 4, the current theory, which suggests the scaling form $2W/Q^{3/2}$, also removes the reported discrepancies between the (110) and (220) results.

In summary, we have shown that the two-line shape diffraction profile and its dependence upon film thickness can be understood quantitatively within the Krivoglaz x-ray scattering theory. We demonstrated that the thin-film two-line shape profile converges for thicker films to the well-known Bragg broadening, caused by bulk dislocations. The detailed measurement and the analysis of extended diffuse scattering maps in Nb/Al_2O_3 give unambiguous evidence of a dislocation network of type B and of a minority presence of secondary dislocations of type A.

The authors are grateful to HASYLAB for continuous support and assistance during the time the experiments were being carried out.

[1] P. M. Reimer, H. Zabel, C. P. Flynn, and J. A. Dura, Phys. Rev. B **45**, 11426 (1992).
[2] A. R. Wildes, R. A. Cowley, R. C. C. Ward, M. R. Wells, C. Jansen, L. Wireen, and J. P. Hill, J. Phys.: Condens. Matter **10**, L631 (1998).
[3] G. L. Zhou and C. P. Flynn, Phys. Rev. B **59**, 7860 (1999).
[4] G. Gutekunst, J. Mayer, and M. Rühle, Philos. Mag. A **75**, 1357 (1997).
[5] P. F. Miceli and C. J. Palmstrom, Phys. Rev. B **51**, 5506 (1995).
[6] P. F. Miceli, J. Weatherwax, T. Krentsel, and C. J. Palmstrom, Physica B **221**, 230 (1996).
[7] M. Huth and C. P. Flynn, Appl. Phys. Lett. **71**, 2466 (1997).
[8] V. M. Kaganer, R. Kohler, M. Schmidbauer, R. Optiz, and B. Jenichen, Phys. Rev. B **55**, 1793 (1997).
[9] M. Krivoglaz, *Diffuse Scattering of X-Rays and Neutrons by Fluctuations*, edited by S. Moss, J. Peisl, V. Baryakhtar, and M. Ivanov (Springer, Berlin, 1996).
[10] J. Hirth and J. Lothe, *Theory of Dislocations* (Springer, New York, 1968).
[11] L. D. Landau and E. M. Lifshitz, *Theory of Elasticity* (Pergamon, Oxford, 1959).
[12] In our calculation image forces which have a form analogous to Eq. (5) have been introduced.
[13] B. E. Warren, *X-Ray Diffraction* (Dover, New York, 1969).

Downloaded 06 Sep 2009 to 160.91.157.167. Redistribution subject to AIP license or copyright; see http://apl.aip.org/apl/copyright.jsp